Micromechanics of Agglomeration Forced by the Capillary Bridge: The Restitution of Momentum

Boris V. Balakin, Sergey Alyaev, Alex C. Hoffmann, and Pawel Kosinski
Dept. of Physics and Technology, University of Bergen, Allegaten 55, 5007 Bergen, Norway

DOI 10.1002/aic.14162
Published online June 21, 2013 in Wiley Online Library (wileyonlinelibrary.com)

The formation of capillary bridge formed by a liquid adsorbate is one of the main reasons for agglomeration in multiphase flows. Agglomeration takes place when the relative momentum of two colliding particles is fully consumed by the bridge. This article presents a theoretical study of the collisions of particles with adsorbed liquid taking into account the influence of capillary and viscous dissipative forces. The article proposes an approximate analytical solution for the dynamics of the bridge formed during the collision, together with a more complete numerical model, which is validated with experimental data. The restitution of the relative momentum of the colliding particles, depending on a series of dimensionless parameters characterizing the bridge, is investigated. A criterion for prediction of agglomeration, or "collision efficiency," in a flow involving cohesive particles is given. An expression is proposed for the coefficient of restitution for the case of collision via a liquid bridge. © 2013 American Institute of Chemical Engineers *AIChE J*, 59: 4045–4057, 2013

Keywords: flocculation, multiphase flow, liquid bridge, capillary number, coefficient of restitution

Introduction

Multiphase flows involving solid particles are encountered in a huge variety of terrestrial and celestial phenomena. They are often strongly influenced by in-phase, particle–particle interactions which lead to loss of relative particle momentum and, in many cases, to the formation of agglomerates. There are two main mechanisms of agglomeration in multiphase flows: molecular interactions of van-der-Waals type and capillary-driven attraction of particles.[1] The latter is the stronger and more variable in terms of cohesivity, something that provides the opportunity for artificial control of the process. For example, granulation[2,3] can be enhanced by variation of the wettability of the particles and the droplet size of a binder (the bridging fluid).[4] Conversely, the presence of repulsive interaction arising from constituents in the carrier phase may lead to a reduction of otherwise expected hydrate plugging in the petroleum industry.[5–7]

In order to accurately model such effects it is important to quantify the amount of relative momentum lost due to the presence of a liquid bridge during an interparticle collision. This analysis can be done by considering the forces acting within the bridge on colliding particles. In general such an analysis must, in part, resort to (semi-) empiricism, since there are no analytical expressions available for some of the involved processes.

The attractive force acting on two stationary spherical particles connected by a liquid bridge generally depends on the wettability of the particle surfaces for the bridging liquid, the interfacial tension of the bridging liquid with the surrounding medium, the volume of the bridge and the interparticle separation distance. The main source of uncertainty in most existing expressions for this force comes from the fact that it is strongly related to the curvature of the interface between the liquid bridge and the surrounding, carrier media. Mazzone et al.[8] related the force between two particles in relative movement to a complex function of the so-called filling angle (α in Figure 1). However, their analytical study was based on empirical determination of this angle. The filling angle, in general, depends also on the dynamics of the bridge, which makes it difficult to use the empirical expression used by Mazzone et al.,[8] for the general case.

The so-called "gorge" method was invoked by Pitois et al.[9] The technique is based on a circular approximation to the bridge surface profile and estimates the capillary force with 10% accuracy compared to numerical simulations. The Laplace-Young equation was solved numerically by Mikami et al.[10] varying a number of dimensionless factors, which influence the bridging force. Their numerical results were then used for an exponential approximation of the force. This expression involves, among other things, the filling angle, which is not known *a priori* in their modeling approach.

An extensive approach was developed by Rabinovich et al.[11] based on the book of Israelachvili, 1992.[12] The force is this case is considered to be equal to the derivative of the energy of the bridge. The resulting expression for the bridging force also involves the filling angle and Rabinovich et al.[11] proposed a differential equation (DE) for determination of this angle, the equation relating the angle to the separation distance. Moreover, the authors studied the asymptotic cases for short separation distances (of the order of

Correspondence concerning this article should be addressed to B. V. Balakin at Boris.Balakin@ift.uib.no.

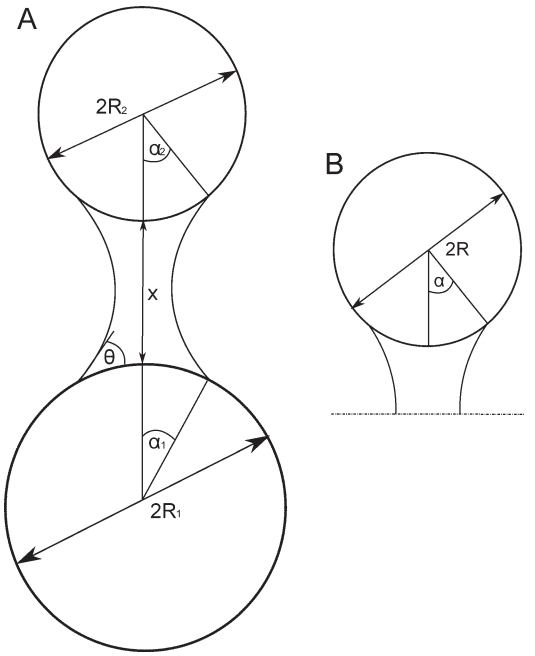

Figure 1. Schematic representation of the liquid bridge system.

(A) two unequal particles within a bridge. (B) equivalent size system

nanometers) and large separations (hundreds of microns). The analytical solutions of Rabinovich et al.[11] agree well with experimental micromechanical force measurements and are evaluated for use as the basis for the work in this article.

It has to be noted that all of the above-mentioned expressions for the liquid bridging force between two particles are derived assuming the particles to be identical spheres.

We now turn to a discussion of dynamic bridging during particle collisions. In contrast with the static case, the movement of particles is always accompanied by a viscous dissipative force acting in the bridge due to lubrication of the particle surface with the fluid between them.[1] An expression for the viscous force is often found from the solution of the Navier-Stokes equations in the gap between the spheres[13] via the integration over the sphere surface of the pressure acting between the particles due to the viscous flow of the fluid between the particles. However, the expression for the force resulting from this integration is hyperbolic with respect to the separation distance and, therefore, has a singular point for the limit of small separation. It is therefore not fully suited for use. Most researchers who applied expressions with singular points for viscous forces,[8,14,15] in the analysis of the bridge mechanics assume a finite minimum separation distance. A physical meaning is often assigned to this distance with reference to roughness of the surfaces of the particles.

Mazzone at al., 1987[8] considered three expressions for the dissipative force, two of which have a singularity on contact. The third expression, originally derived by Jen and Tsao,[16] relates the viscous force to the filling angle; this makes the viscous force decay faster than the conventional hyperbola. The work by Zhang et al.[17] should also be mentioned when discussing the issue of a singularity in the viscous force on contact. Zhang et al.[17] succeeded in avoiding the "contactless paradox" by including van-der-Waals interaction into the balance of forces during collision, what made it possible to reduce the minimum separation distance to the nanoscale, below the molecular size of the lubricating material. In spite of these efforts to overcome the problem of a singularity in the viscous force on contact, the current state-of-the-art on viscous force modeling leads to the conclusion that there is a need for better modeling of the force using molecular dynamics and computational fluid dynamics (CFD).

The literature discussed above shows the characterization of bridge-dominated particle collisions to be complex. Experimental work aimed at elucidating such collisions often measures the restitution of momentum after the collision of a particle on an object (sphere or plane) covered with a liquid film, but generally does not attempt to relate this to the dynamics of the fluid within the bridge formed.

The work by Gollwitzer et al.[18] reports the results of high-speed video tracking of the collision of spheres with a plane covered by a liquid film. The normal restitution coefficient was defined as the ratio between particle velocities normal to the wall after and before the collision. The normal restitution coefficient was found to depend on the initial approach velocity, the thickness of the liquid film, the bridge material, the particle size, and the particle Stokes number. The number of parameters influencing the process was not reduced by their organization into dimensionless groups (except for the Stokes number). Moreover, although the dependence of the restitution coefficient on the nature of the liquid making up the film was studied, no explicit dependencies on the viscous dissipative force acting in the bridge or the wettability of the particle surface to the bridging liquid were taken into account. The experiment by Antonyuk et al.[15] and a subsequent numerical study by Jain et al.,[19] consider the dependence of the restitution coefficient on the thickness of the liquid film, the particle approach velocity, and the viscosity of the film. The authors of these articles[15,19] additionally propose a set of theoretical models for the mechanics of the particle, which agree well with the experiment.

The spheres used in experiments[15,18,20] were large (of the order of millimeters) compared to the particles involved in most applications what made the process studied to be inertia-dominated.[21]

A complete theoretical and experimental study of liquid bridge dynamics was done by Mazzone et al.[8] They studied the rupture of the bridge located between two steel spheres of which one was fixed and the second adhered to the first by means of magnetization. At the beginning of each experiment the magnetic field was removed from the system and the free particle detached from the bridge by gravity. Microscopic video tracking of the process was performed to record the displacement of the second sphere, the shape, and the filling angle of the bridge as functions of time. The experiment was performed using different bridging liquids, thus, altering the wettability of the surfaces to the bridging liquid and the viscosity in the bridge. A theoretical model for the particle mechanics was proposed with use of an empirically based expression for the liquid bridge force, mentioned above, and three different expressions for the viscous dissipative force. The model was nondimensionalized and solved numerically, demonstrating good agreement with experimental data.

It was found among other things that the model results strongly depend on the minimum separation distance, that is, the model is sensitive to the initial condition. Another

important observation was that the filling angle was not significantly changed with separation for the bridges studied experimentally. That led the authors[8] to apply the viscous dissipative force proposed by Jen and Tsao,[16] with a fixed filling angle, which eliminated the singularity in the model. The viscous force by Jen and Tsao,[16] demonstrated suitable agreement with experiment for rather viscous bridges ($\mu = 0.125$ Pas and $\mu = 12.5$ Pas). The work by Mazzone et al.[8] is relevant to the aim of this study, but not entirely so, since their work mainly deals with the separation process taking place after the contact of colliding particles and does not consider their approach. In addition, the article does not consider the case when the particles form an agglomerate under the influence of the liquid bridge. Nevertheless, the experimental data produced in the work of Mazzone et al.[8] are used for validation of the approach in this article.

The article by Wang et al.[22] studying the separation of particles is highly relevant to this work. The authors developed a theoretical model for the dynamics of the particles and the liquid in a connecting bridge during the separation. They considered the superposition of a liquid bridging force, a viscous force, the detachment force applied to the particles and gravity as governing the process. The equation of motion for the particles under the influence of these forces was solved numerically and the process was studied in terms of the time of separation. This parameter implicitly determines the collisional restitution of momentum.

In terms of basic physical parameters, the above-mentioned forces, and, therefore, the time of separation, was considered to depend on: the mass and radius of the particle(s), the minimum separation distance, the surfaces' wettability to, and the viscosity of, the bridge liquid and the volume of the bridge. Rupture of the bridge is considered to take place when the sum of the capillary force, the dissipative force and the gravitational force reduces to 90% of the detachment force. This percentage is selected arbitrarily and no physical reason is given for this choice. The outcome of the resulting model is in line with expectation and stands to reason. Although the equation of particle motion was nondimensionalized, the influences of the parameters are presented in dimensional form increasing the number of parameters. The approach of the particles before collision and bridge-driven agglomeration are not considered, as in the work of Mazzone et al.[8]

In light of the above it can be concluded that the process of bridge-dominated particle–particle and particle–wall collisions is not yet completely described in the research literature. In particular:

- there is a lack of information on the processes taking place during the approach to collisions,
- there is a need for description of the process leading to agglomeration of the colliding particles, and finally
- there is a need for the derivation of a consistent set of nondimensional parameters governing the process.

Furthermore, recent articles on this subject[8,15,22] describe numerical solutions of the equations for particle motion when a bridge is present, this article will show that it is also possible to work out an approximate analytical solution for the particle motion.

This article considers the movement of two particles connected by a liquid bridge during the stages of precollisional approach and postcollisional separation (until rupture of the bridge). In addition to the capillary and viscous forces taken into account in other articles, an external force is included into the equation of motion here, which would mimic a possible influence from the flow of the carrier phase, gravity, or any other external force. The model will be solved numerically and validated against the experiments of Mazzone et al.[8] The model considers only the components of the particle velocities that are normal to the plane of collision.

A slight simplification of numerical model makes it possible to find an approximate analytical solution for the coefficient of restitution of the particles. A criterion for the bridge-dominated agglomeration of colliding particles is proposed. Finally, the analytical expression for the coefficient of restitution is used for the formation of a semiempirical function which approximates the results of the numerical model, and in this way the range of applicability of the limited analytical solution is expanded into that of the numerical model and an expression that can easily be implemented in simulations is obtained.

Theoretical Approach

Geometry

A two-dimensional schematic representation of a typical liquid bridge between two unequal spheres with the radii R_1, R_2 and masses m_1, m_2 is shown in Figure 1A. It is assumed that the bridge is axially symmetric. The filling angles α_1 and α_2 are indicated in the figure and represent the spread of the bridge over the surface of the spheres. These angles can be seen as spherical coordinates in two coordinate systems with origins at the centers of the particles. In this article, it is assumed that the particles are of the same material so the wetting angle θ is equal for both of them. The spheres are separated from each other by distance x.

The analytical expressions for forces acting within the bridge used in here do not account for the particle sizes to differ. Following previous work by these authors,[23] the geometry is simplified to a system where a particle of an equivalent size, defined as $R=\frac{R_1R_2}{R_1+R_2}$ is considered to move normally to a symmetry plane.

Also, an equivalent filling angle is defined as: $\alpha=\frac{\alpha_1\alpha_2}{\alpha_1+\alpha_2}$ and an equivalent particle mass, $m=\frac{m_1m_2}{m_1+m_2}$, while the definition of the wetting angle θ is kept unchanged. The equivalent system is depicted in Figure 1B.

Forces

It is assumed that the forces acting on the particles in the direction normal to the symmetry plane dominate relative to possible forces acting in the tangential direction. Two different force diagrams are shown in Figure 2. In the approach scenario, the particles enter the bridge with an initial normal velocity v_0^A. The liquid bridging force is directed towards the symmetry plane and is, according to Rabinovich et al.,[11] given by

$$F_c=-\frac{2\pi R\gamma\cos\theta}{1+\frac{x}{2d_{sp}}}-2\pi R\gamma\sin\alpha\sin(\theta+\alpha), \tag{1}$$

where γ is the surface tension of the bridge liquid. d_{sp} is the height of the spherical cap on the sphere surface covered by the liquid bridge[11]

$$d_{sp}=\frac{x}{2}\cdot\left(-1+\sqrt{1+2V/(\pi Rx^2)},\right) \tag{2}$$

where V is the volume of the liquid bridge.

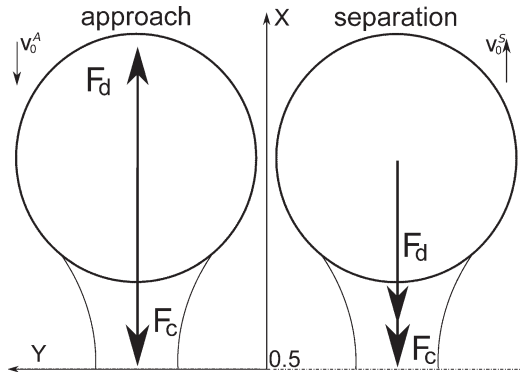

Figure 2. Forces acting on a particle with a bridge.

The external force $\vec{F}_{ext}$ is not shown and can be directed in either of the two normal directions.

The dissipative viscous force always acts against the direction of particle movement and may be given by[8]

$$F_d = -3\pi\mu R^2 \frac{1}{x}\frac{dx}{dt}, \tag{3}$$

where μ is the bridge dynamic viscosity. This expression was originally derived for the viscous force acting between two particles colliding in a homogeneous fluid. The lubrication approximation was applied to derive Eq. 3 so it is valid for $Re \ll 1$.

During the contact, the particles normally lose part of their mechanical energy in a collision which may be described by a classical restitution coefficient. The relative particle velocity just after the contact v_0^S is taken as an initial condition for the separation scenario, the separation scenario leading to either rupture of the bridge or particle agglomeration. During the separation, the liquid bridging force, F_c, acts in the same direction as during the approach. However, since the relative velocity has changed direction, the dissipative force, F_d, during separation acts in the same direction as F_c.

As mentioned, the presence of a constant external force, F_{ext} acting along the line connecting the particle centers but of arbitrary magnitude is also taken into account, this force is not shown in Figure 2.

General model

The equation of the particle motion is defined by Newton's second law as

$$m\frac{d^2x}{dt^2} = F_c + F_d + F_{ext}. \tag{4}$$

Substituting for F_c and F_d from Eqs. 1–3, Eq. 4 becomes a nonlinear DE of the second order. The dimensionless separation distance $\xi = \frac{x}{R}$, time $\tau = \sqrt{\frac{\pi\gamma}{m}}t$, and bridge volume $\hat{V} = \frac{V}{\pi R^3}$ are substituted into Eq. 4 and the equation is then scaled with $\pi R\gamma$ to make it dimensionless.

$$\frac{d^2\xi}{d\tau^2} = \hat{F}_c + \hat{F}_{dd} + \hat{F}_{ext} \tag{5}$$

It has to be also noted that the procedure to obtain the dimensionless Eq. 5 is different from that followed by Mazzone et al.[8] who scaled the equation of motion with the external force $F_{ext} = mg$. The present approach is able to account for cases when there is no external force acting on the particles. Although the volume of the bridge is formally dependent on the wetting angle θ the current model treats these variables as they would be mutually independent. The dimensionless dissipative force is therefore reduced to

$$\hat{F}_d = -C_a \frac{\frac{d\xi}{d\tau}}{\xi} \tag{6}$$

where $C_a = \frac{3\mu v^*}{\gamma}$ is the capillary number of the bridge. The characteristic velocity

$$v^* = \sqrt{\frac{\pi R^2\gamma}{m}} \tag{7}$$

can be seen as the velocity that an initially stationary particle of mass m and radius R would attain if subjected to the work of a capillary force of $\gamma\frac{R}{2}$ over the distance of πR.

d_{sp} in the expression for F_c can be related to the filling angle by (see Figure 1B)

$$d_{sp} = R - R\cos\alpha \approx R\frac{\alpha^2}{2}. \tag{8}$$

Following Rabinovich et al.,[11] the volume of the bridge is given by

$$\hat{V} = \alpha^2\xi + 0.5\alpha^4. \tag{9}$$

$\hat{V}$ is constant due to volume conservation of the bridge. Taking the full derivative of $\hat{V}$, setting it equal to zero and solving the resulting equation for $d\alpha/d\xi$ leads to a DE

$$\frac{d\alpha}{d\xi} = \frac{-1}{\frac{2\xi}{\alpha} + 2\alpha}, \tag{10}$$

which is solved analytically (the integration constant is found from Eq. 9)

$$\alpha = \sqrt{-\xi + \sqrt{\xi^2 + 2\hat{V}}}. \tag{11}$$

Taking into account, Eqs. 8 and 11 leads to the final expression for the dimensionless liquid bridging force

$$\hat{F}_c = -\frac{2\cos\theta}{1 + \frac{\xi}{\sqrt{\xi^2+2\hat{V}}-\xi}} - 2\sin\sqrt{-\xi+\sqrt{\xi^2+2\hat{V}}}\sin \times\left(\theta + \sqrt{-\xi+\sqrt{\xi^2+2\hat{V}}}\right). \tag{12}$$

This, then, consitutes an expression for the dimensionless bridging force as a function only of the dimensionless separation. This expression is given in another form in Rabinovich et al.[11]

The order of Eq. 5 can be reduced by the substitution: $v = \frac{d\xi}{d\tau} = \frac{v}{v^*}$ to give

$$v\frac{dv}{d\xi} + \frac{2\cos\theta}{1 + \frac{\xi}{\sqrt{\xi^2+2\hat{V}}-\xi}} + 2\sin\sqrt{-\xi+\sqrt{\xi^2+2\hat{V}}}\sin \times\left(\theta + \sqrt{-\xi+\sqrt{\xi^2+2\hat{V}}}\right) + C_a\frac{v}{\xi} - \frac{F_{ext}}{\pi R\gamma} = 0. \tag{13}$$

Equation 13 is general for both approach and separation, however its initial conditions are different: $v(\xi_{max}) = v_0^A < 0$ for approach, $v(\xi_{min}) = v_0^S > 0$ for separation. ξ_{min} is the minimum possible separation distance, a parameter required in

the expression for $\hat{F}_d$, which is singular at $\xi=0$. This parameter is varied during the simulations in the interval (0.002, 0.01), which was selected taking into account minimum separations used in Ref. 8 and [24]. Physically, ξ_{min} can be attributed to the roughness of the particle surface.

The maximum separation distance, which is the separation whereby the bridge ruptures, is determined by the amount of liquid in the bridge, that is, the bridge volume. The bridge ruptures due to Rayleigh—Plateau instability.[25] According to literature this maximum separation is proportional to the cubic root of the bridge volume and is also a function of the wetting angle, θ. In addition, Pitois et al.[9] have demonstrated that, in the dynamical case, this distance also depends on the velocity of separation

$$\xi_{max}=(1+0.5\theta)\left(1+(C_{a0})^{\frac{1}{2}}\right)\cdot\hat{V}^{\frac{1}{3}} \tag{14}$$

where $C_{a0}=\frac{C_a v_0}{3}$. According the work by Megias-Alguacil and Gauckler,[25] experiments confirm that rupture occurs at distances in between the ones predicted by Eq. 14 for the static condition (i.e., $C_{a0}=0$) and those corresponding to the criterion for Rayleigh—Plateau instability

$$\xi^{R-P}\approx 2\pi\sin\alpha \tag{15}$$

Equation 14 can be seen as a semiempirical expression for ξ_{max} for the dynamic case. Equation 14 is used in this work both for formation of the bridge at approach and for the rupture of the bridge on separation, similarly to Lian et al. and Darabi et al.[24,26] This is an approximation since in reality the bridge will form at lower separations, whereby the adsorbed layers on the particles almost touch. Another comment is that the initial separation velocity is used here, where the velocity at bridge rupture should be used. This means that the separation corresponding to rupture will be overestimated.

Equation 13 is an Abel equation of the second kind,[27] which, in this form, does not have an exact analytical solution. It was solved numerically using the well-known fourth order Runge-Kutta technique.

To make this procedure simpler, backward substitution of $v=\frac{d\xi}{d\tau}$ into Eq. 13 was done to bring it back to its original higher-order form, represented by Eq. 5. The dimensionless time step was set to $0.1\text{ns}\times\sqrt{\frac{\pi\gamma}{m}}$.

Approximate, analytical model

Equation 13 can be simplified to formulate an approximate analytical solution by making a number of assumptions about the geometry of the liquid bridge and the capillary force.

Figure 3 presents a rough approximation of the bridge geometry at different stages of the collision. At the point of contact (in the vicinity of ξ_{min}) the separation is minimal $x_{min}=\xi_{min}R$ and the filling angle is maximal, α_{max}. The volume of the bridge can be roughly approximated by the volume of two equal cones

$$V=\pi R^3\sin\alpha_{max}{}^2\frac{\xi_{min}}{3} \tag{16}$$

where $\sin(\alpha)$ has been approximated by α for large separation where α is small. This assumption does not account for possible change of the shape of the bridge due to bursting of the liquid from the gap near the point of contact.

This gives for the value of the maximum filling angle

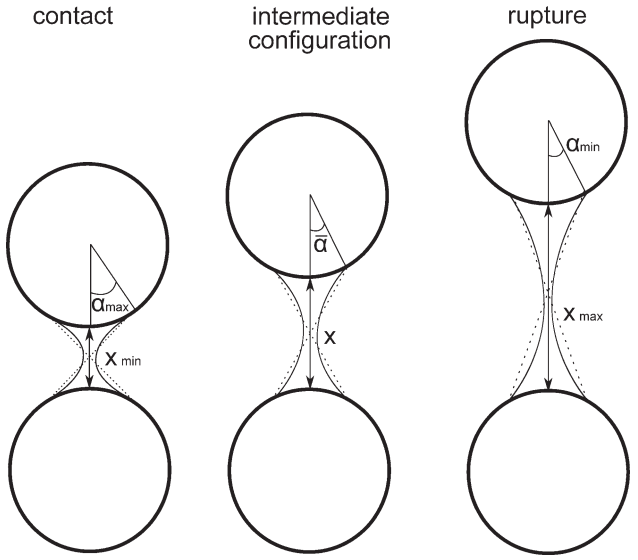

Figure 3. Assumed approximation of the bridge geometry.

$$\alpha_{max}=\sqrt{\frac{3\hat{V}}{\xi_{min}}} \tag{17}$$

The minimum filling angle is derived in similar way

$$\alpha_{min}=\sqrt{\frac{3\hat{V}}{\xi_{max}}} \tag{18}$$

Supported by the observation by Mazzone et al.,[8] it is proposed that α varies gently and monotonically during the process. Linear interpolation gives an approximate intermediate or mean value

$$\bar{\alpha}=\frac{1}{2}(\alpha_{min}+\alpha_{max}) \tag{19}$$

Analogous to the approach shown in Eq. 16, the mean value of the bridge volume is then related to the separation distance as follows

$$\hat{V}=\frac{1}{3}\bar{\alpha}^2\xi. \tag{20}$$

According to Rabinovich et al.,[11] for large separation distances $\xi_{min}\gg\sqrt{\hat{V}}$ the expression for the liquid bridging force can be simplified to:

$$\hat{F}_c=\frac{-2\hat{V}\cos\theta}{\xi^2} \tag{21}$$

The conical approximation of the bridge geometry makes the estimation of the equivalent hydraulic radius of the bridging gap, $d_{eq}=2R\sin(\alpha)$. This makes it possible to derive a critical Reynolds number for the flow in the bridge at the maximum interparticle velocity $Re=\frac{2R\sin(\alpha_{min})\rho v_0^A}{\mu}=1$. The expression for the dimensionless approach velocity, $v_0^A=v_0^A/v^*$ for which the dissipative force is valid becomes

$$v_0^A<\frac{1}{2\sin(\alpha_{min})Re^*} \tag{22}$$

where $Re^*=\frac{\rho R v^*}{\mu}$.

Making use of Eqs. 20 and 21, the equation of the motion of particles (13) becomes:

$$v\frac{dv}{d\xi} = -\frac{1}{\xi}\left(\frac{2\bar{\alpha}^2\cos\theta}{3} + C_a v\right) + \frac{F_{ext}}{\pi R\gamma} \tag{23}$$

where $\bar{\alpha}$ is given by Eq. 19.

While in the work of Mazzone et al.,[8] an external force, F_{ext}, played an important role in pulling the particles apart, this work focuses on collisions where the particle momentum constitutes the driving force for approach and separation. The external force can therefore be neglected in many contexts in this work (but not all, see below). Neglecting F_{ext} makes an analytical integration of Eq. 23 possible

$$K + \frac{C_a v - \phi\ln(C_a v + \phi)}{C_a^2} = \ln\frac{1}{\xi} \tag{24}$$

where K is the constant of integration which may be found from the initial conditions and $\phi = \frac{2}{3}\bar{\alpha}^2\cos\theta$ was substituted into Eq. 23 before solving it for simplicity. This equation applies to both approach and separation.

Equation 24 expresses the dependence of the dimensionless velocity, v, on the dimensionless separation distance, ξ, in an implicit form. Using the initial condition $\left(v = v_0^A\right)|_{\xi=\xi_{max}}$ for approach and $\left(v = v_0^S\right)|_{\xi=\xi_{min}}$ for separation and solving for the relative velocity divided by the initial one, v/v_0, gives:

$$\frac{v}{v_0^A} = -\frac{\phi}{C_a v_0^A}\left[W_0\left(-\exp\left[\ln\left(\frac{C_a v_0^A}{\phi}+1\right) + \frac{C_a^2}{\phi}\ln\left(\frac{\xi}{\xi_{max}}\right) - \frac{C_a v_0^A}{\phi} - 1\right]\right) + 1\right] \tag{25}$$

for approach and

$$\frac{v}{v_0^S} = -\frac{\phi}{C_a v_0^S}\left[W_{-1}\left(-\exp\left[\ln\left(\frac{C_a v_0^S}{\phi}+1\right) - \frac{C_a^2}{\phi}\ln\left(\frac{\xi_{min}}{\xi}\right) - \frac{C_a v_0^S}{\phi} - 1\right]\right) + 1\right] \tag{26}$$

for separation, where W is the Lambert W-function (see e.g., Ref. 28) and subscripts 0 and -1 indicate the chosen branch of the function. The branches of W for approach and separation are chosen to give physically meaningful results for Eq. 24. In order to achieve an approximation in terms of simple functions we utilize the logarithmic series.

For approach approximating W_0 in Eq. 25 by the first two terms of its logarithmic expansion for large values of the argument, as it is shown in Ref. 28, gives:

$$\frac{v}{v_0^A} = 1 - \frac{\phi}{C_a v_0^A}\ln\left[-\left(\frac{C_a v_0^A}{\phi}+1\right)\right] - \frac{C_a}{v_0^A}\ln\left(\frac{\xi}{\xi_{max}}\right) + \frac{\phi}{C_a v_0^A}\ln\left[\ln\left(-\left(\frac{C_a v_0^A}{\phi}+1\right)\right) + \frac{C_a^2}{\phi}\ln\left(\frac{\xi}{\xi_{max}}\right) - \frac{C_a v_0^A}{\phi} - 1\right]. \tag{27}$$

For separation, truncation of the logarithmic expansion of W_{-1} after two terms gives the following approximation of Eq. 26 (see e.g., Ref. 29)

$$\frac{v}{v_0^S} = 1 - \frac{\phi}{C_a v_0^S}\ln\left(\frac{C_a v_0^S}{\phi}+1\right) + \frac{C_a}{v_0^S}\ln\left(\frac{\xi_{min}}{\xi}\right) + \frac{\phi}{C_a v_0^S}\ln\left[-\ln\left(\frac{C_a v_0^S}{\phi}+1\right) + \frac{C_a^2}{\phi}\ln\left(\frac{\xi_{min}}{\xi}\right) + \frac{C_a v_0^S}{\phi} + 1\right]. \tag{28}$$

Results and Discussion

Validation of models

The model represented by Eq. 13 and evaluated numerically was validated against the experimental data presented in Mazzone et al.[8] for two bridging liquids, one with high surface tension and the other with high viscosity. These were dibutylphtalate (DBT) ($\gamma = 3.22 \cdot 10^{-2}$ N/m, $\mu = 0.014$ Pas) and silicon immersion oil ($\gamma = 2.55 \cdot 10^{-2}$ N/m, $\mu = 1.25$ Pas), respectively.

The former system, using DBT, is thus capillary-force dominated while the latter is dominated by the viscous force. The dimensionless parameters in Eq. 13 were computed with the use of data given in Mazzone et al.[8] They are listed in the caption of Figure 4. The minimum separation distance ξ_{min} was selected as the one resulting in optimal agreement with the results in Ref. 8.

Figure 4 shows the dimensionless separation distance, ξ, as a function of dimensionless time, τ_M, for DBT and immersion oil predicted by the present model (Eq. 13) compared with the experiments by Mazzone et al.[8] In order to compare the two, dimensionless time used in this figure is defined as it is in the work,[8] this is related to the dimensionless time used in this work via the expression

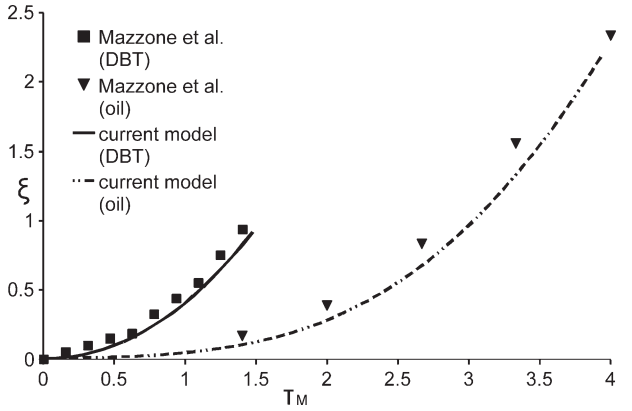

Figure 4. Rupture of a liquid bridge between solid spheres under the influence of gravity. Dimensionless separation distance as a function of dimensionless time.

Model results are compared with the experimental results of Mazzone et al.[8] for DBT and silicon immersion oil. Dimensionless time is, in this figure, defined as in Mazzone et al.,[8] which is related to the our scaling through the expression $\tau_M = \tau\sqrt{F_{ext}}$. Parameters: $\theta = 10^\circ$, $\xi_{min} = 0.005$, $V = 0.04$, $v_0^S = 0$ Parameters specific for the liquids: DBT: $F_{ext} = 12.48$, $C_a = 0.0515$ Oil: $F_{ext} = 15.76$, $C_a = 5.1695$

$$\tau_M = \tau\sqrt{\hat{F}_{ext}} \tag{29}$$

As seen from Figure 4, the separation between the particles is much slower in the viscous-force dominated case. The agreement between the experiments and the model is very good, even though the two cases are so different. The fact that the model slightly underpredicts the experimental data could be explained by the bridging force being calculated using a value of α (Eq. 11) found from an approximated bridge curvature (the bridge surface assumed parabolic according to Eq. 9).

The expression for the rupture distance given in Eq. 14 is widely quoted in the literature.[1,9,10] However, for the experiments by Mazzone et al.[8] this relation returns $\xi_{max}^{DBT} = \xi_{max}^{oil} \approx 0.037$, which is significantly lower than the values obtained experimentally. Equation 15, the criterion for Rayleigh—Plateau instability, returns more accurate estimate for the present system $\xi^{R-P} \approx 2.65$. Both the theoretical model (Eq. 13) and the approximate one (Eq. 28) are able to account a maximum separation distance as a parameter, irrespectively of the way it is quantified.

It can thus be concluded that the numerical model is sufficiently accurate for quantitative predictions. The next stage is to validate the approximated analytical solution, given by Eqs. 27 and 28, by comparing it with the numerical model for the case when $\hat{F}_{ext} = 0$.

This comparison was done for the type of conditions which can be met in, for example, the petroleum industry. 100 μm spherical particles were considered to be connected by an aqueous bridge of 1.0×10^9 $(nm)^3$ and to have an initial relative velocity of 0.01 m/s (equal for both approach and separation, this is, therefore, not meant to represent approach and separation for the same collision). The values of the dimensionless criteria are shown in the caption of Figure 5. These figures show the evolution of the separation distance with time and the relative particle velocity as a function of separation distance during the processes of approach and separation.

Although the particles are attracted by the bridge force, the effect of the dissipative force is clearly seen during the approach where the particles lose approximately 33% of their normal momentum relative to the plane of impact. The mechanical contact of particles occurs at ξ_{min} with non-zero relative velocity. Some relative momentum could later be lost in the contact collision which followed the stage of approach. If the resulting relative velocity after the contact is non-zero then the stage of the bridge-dominated separation begins. Up to 40% of momentum has been lost during the separation as the liquid bridge force acts in the direction opposite to the relative particle motion at this stage and therefore in the same direction as the viscous force. $\xi_{min} = 0.005 \gg \sqrt{\hat{V}}$ so the approximated analytical model is valid for this case. It agrees well with the exact numerical solution lending the credence to the present approach.

The influence of an external force was studied using the numerical model, which, as mentioned, in contrast to the approximate analytical solution, is able to take this force into account.

The influence of an external force in the numerical model is shown in Figure 6. In this example, the parameters of the process used are the same as in Figure 5, that is, this is a case where, in the absence of an external force, the particles do not agglomerate. When the external force is acting in the direction of the initial relative velocity, the particles are accelerated to above the initial relative velocity during both approach and separation. The restitution exceeds unity in this case. Conversely, when the force acts in the opposite direction to the relative particle motion the particles, in this example, start to move away from each other before they contact at ξ_{min}. Additional numerical studies of the approach case have shown that an external force is the only mechanism which can cause repulsion without the particles contacting in the present model. The particle is always attracted by the bridge for any $v_0^A \leq 0$.

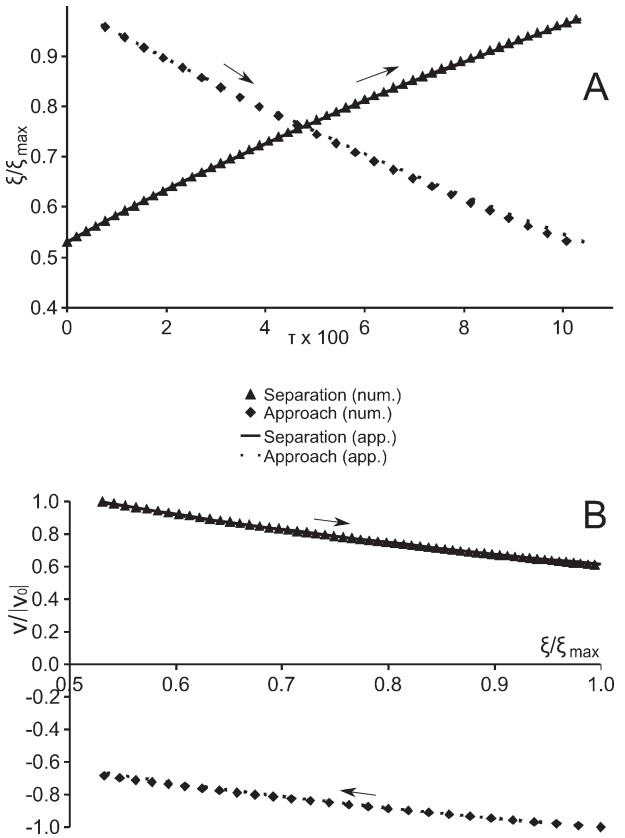

Figure 5. (A) Dimensionless separation distance (scaled with the rupture distance ξ_{max}) as a function of dimensionless time τ; (B) Particle relative velocity (scaled with initial value v_0) as a function of scaled separation distance. Approach and separation scenarios predicted by the numerical model and approximated solution for $\theta = 40^0$, $\xi_{min} = 0.005$, $\hat{V} = 3.19 \cdot 10^{-7}$, $C_a = 0.029$, $\hat{F}_{ext} = 0$, $v_0^A = -0.052$, $v_0^S = 0.052$.

The arrows indicate the direction of particle movement.

Externally forced agglomeration may take place when $\hat{F}_{ext} \leq 0$. This would be agglomeration brought about by the action of an external force for a case where the particles, in the absence of the external force, would be able to escape each other after the collision.

Agglomeration criterion

Agglomeration takes place in case the kinetic energy of the separating particles is not enough to overcome the total work of the potential and dissipative resistance of the bridge.

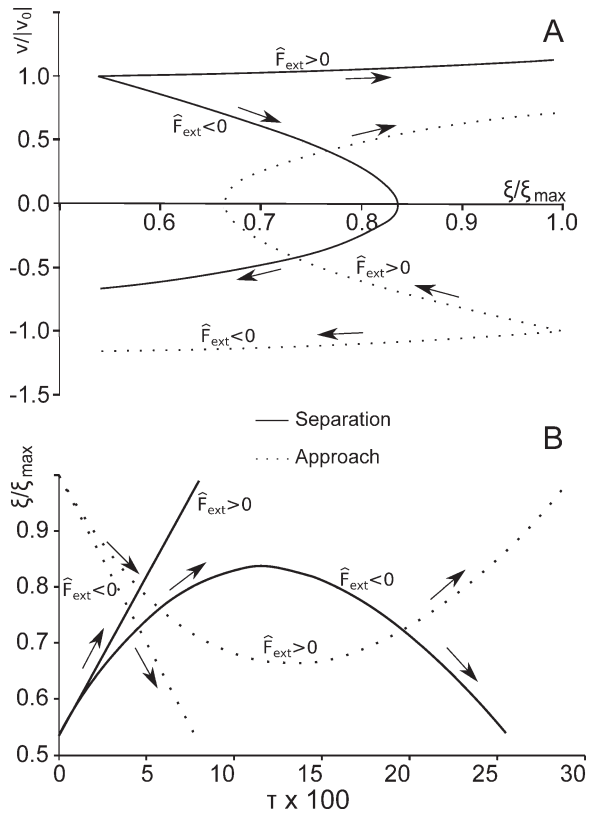

Figure 6. Influence of the direction of an external force on the particle trajectories in terms of: (A) the relative velocity (scaled with initial value v_0) as a function of separation distance (scaled with the rupture distance ξ_{max}); (B) scaled separation distance as a function of dimensionless time τ.

The parameters in the numerical model are: $\theta=40^0$, $\xi_{min}=0.005$, $\hat{V}=3.19\cdot10^{-7}$, $Ca=0.029$, $\hat{F}_{ext}=\pm0.319$, $v_0^A=-0.052$, $v_0^S=0.052$. The arrows indicate the direction of particle movement

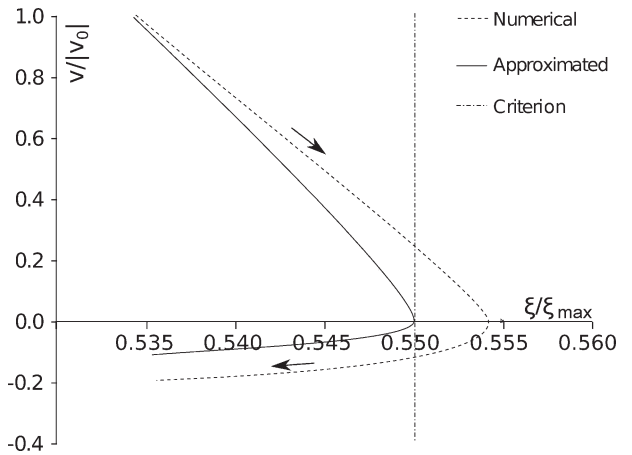

Figure 7. Agglomeration shown as the relative velocity (scaled with initial value v_0) as a function of separation distance (scaled with the rupture distance ξ_{max}).

The prediction of the numerical model is compared with the approximate, analytical solution for $\theta=40^0$, $\xi_{min}=0.005$, $\hat{V}=3.19\cdot10^{-7}$, $Ca=0.1452$, $\hat{F}_{ext}=0$, $V_0^S=5.16\cdot10^{-3}$. Arrows represent the direction of particle movement

This is illustrated in Figure 7, which shows results from a case where the initial relative velocity is lower and the bridge resistance is higher than those in Figures 5 and 6, namely $V_0^S=0.052$ and $C_a=0.1452$, respectively. The numerical solution shows that the relative velocity during separation becomes zero before the bridge ruptures and then changes sign.

As long as $\hat{F}_{ext}=0$ and $\xi_{min}\gg\sqrt{\hat{V}}$, Eq. 24 is a valid model for the collision also if it leads to agglomeration, and this can, therefore, be used to formulate an agglomeration criterion.

Substituting $v=0$ to Eq. 24 and taking into account the initial condition for separation, a critical separation distance is found

$$\xi_{crit}=\exp\left\{\frac{\phi\ln\left(\frac{\phi}{C_a v_0^S+\phi}\right)+C_a v_0^S}{C_a^2}+\ln(\xi_{min})\right\} \quad (30)$$

Equation 30 constitutes a relatively simple criterion for the agglomeration of particles. Agglomeration takes place when $\xi_{crit}\in(\xi_{min},\xi_{max})$. Figure 7 shows that the derived criterion agrees well also with the results of the numerical model.

Loss of momentum due to the viscous force

The fraction of residual relative momentum after the action of the viscous dissipation in the bridge, $\bar{\varepsilon}$, may be defined as $\frac{v(\xi_{min})}{v_0^A}$, $\frac{v(\xi_{max})}{v_0^S}$ for the stages of approach and separation, respectively. This can either be calculated directly from Eqs. 27 and 28 or obtained from the more accurate numerical model given by Eq. 13.

This section reports results of a study of the sensitivity of the fraction of residual relative momentum to variations in the five dimensionless parameters that govern the collision process: Ca, $\hat{V}$, ξ_{min}, $\hat{F}_{ext}$, and θ.

The dependence of the fraction of residual relative momentum on the first of these parameters, the bridge capillary number Ca, is shown in Figure 8 for both the numerical and the approximate analytical solution. Although Ca includes the surface tension in the denominator, it is

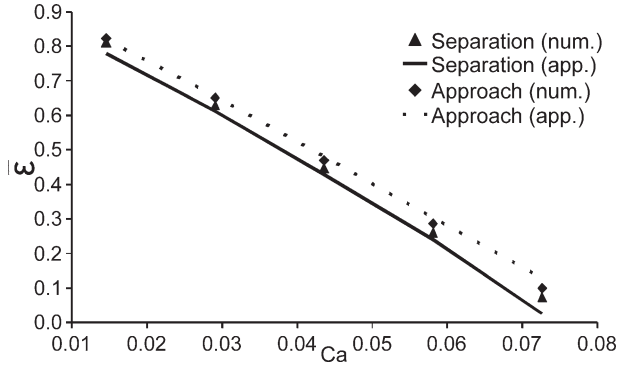

Figure 8. Fraction of residual relative momentum, $\bar{\varepsilon}$, as a function of capillary number Ca. $\theta=40^\circ$, $\xi_{min}=0.005$, $\hat{V}=3.19\cdot10^{-7}$, $\hat{F}_{ext}=0$, $V_0^A=-0.052$, $V_0^S=0.052$.

Numerical results compared with the analytical, approximate solution.

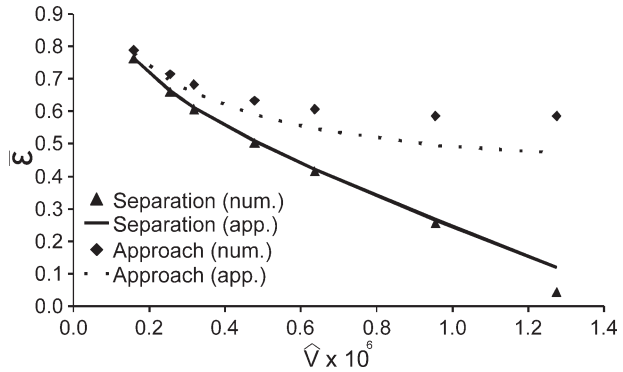

Figure 9. Fraction of residual relative momentum, $\bar{\varepsilon}$, as a function of the bridge volume $\hat{V}$. $\theta=40^0$, $\xi_{min}=0.005$, $Ca=0.029$, $\hat{F}_{ext}=0$, $v_0^A=-0.052$, $v_0^S=0.052$.

Numerical results compared with approximated solution.

essentially a measure of the bridge resistivity to the particle movement. An increase in *Ca* therefore results in a decrease of residual relative momentum for both approach and separation stages. The difference between the analytical and numerical solutions is only slight in this case. The results shown in Figure 8 are in qualitative agreement with results by Wang et al.[22] and Antonyuk et al.[15]

Figure 9 shows the effect of the dimensionless volume of the bridge, $\hat{V}$, on the fraction of residual relative momentum. $\hat{V}$ is a measure of the capillary force and the maximum separation distance via Eq. 14. It is evident that an increase in $\hat{V}$ leads to a reduction in the residual relative momentum for the separation stage, since the attractive force increases with increasing bridge volume.

During the approach the particles are attracted stronger as the bridge volume increases. However, the enhanced attraction accelerates the particle only little since the higher velocity increases the dissipation, which in turn limits the velocity. Moreover, the distance over which the particles lose momentum is also increased due to the increase in ξ_{max} with increasing $\hat{V}$. These factors cause the residual momentum to actually decay with increasing $\hat{V}$. It is conceivable that an increase of the volume outside the interval considered here could increase the residual relative moment for the case of approach.

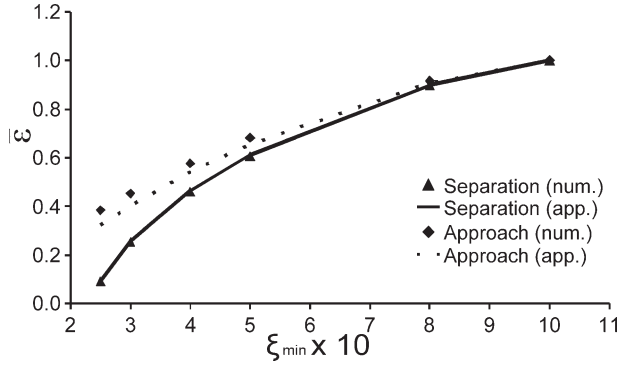

Figure 10. Fraction of residual relative momentum, $\bar{\varepsilon}$, as a function of minimum separation distance ξ_{min}. $\theta=40^0$, $\hat{V}=3.19\cdot10^{-7}$, $Ca=0.029$, $\hat{F}_{ext}=0$, $v_0^A=-0.052$, $v_0^S=0.052$.

Numerical results compared with approximated solution.

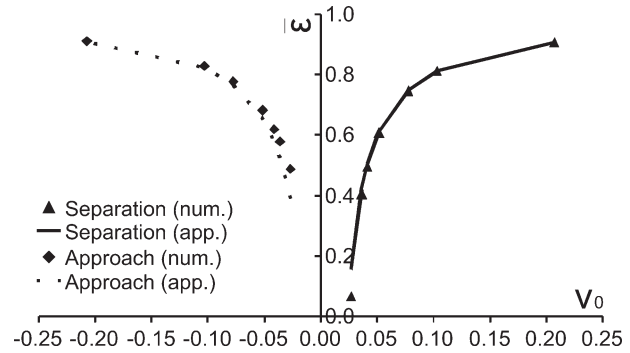

Figure 11. Fraction of residual relative momentum, $\bar{\varepsilon}$, as a function of initial velocity v_0. $\theta=40^0$, $\xi_{min}=0.005$, $\hat{V}=3.19\cdot10^{-7}$, $Ca=0.029$, $\hat{F}_{ext}=0$.

Numerical results compared with analytical, approximate solution.

Since $\hat{V}$ is approximated in the analytical solution, this model is in moderate disagreement with the numerical one for the upper part of the range of volumes tested. Both numerical and analytical results are in qualitative agreement with Wang et al.[22]

The sensitivity $\bar{\varepsilon}$ to the choice of minimum separation distance is shown in Figure 10. As already mentioned, an increase in ξ_{min} decreases the distance over which the viscous force acts. This causes $\bar{\varepsilon}$ to rise with ξ_{min} to asymptotically approach unity at $\xi_{min}=\xi_{max}=1$ as the thickness of liquid layer reduces. The analytical solution agrees well with the numerical one, as seen in the figure. There is a slight discrepancy for small ξ_{min}. The dependence is in the qualitative agreement with Gollwitzer et al.,[18] Antonyuk et al.,[15] and Wang et al.[22]

The influence of initial relative velocity v_0 on $\bar{\varepsilon}$ is shown in Figure 11. The figure shows that an increase in the absolute value of velocity makes the $\bar{\varepsilon}$ increase asymptotically to unity due to the particle inertia. In other words, the fast particle does not "feel" the bridge very much while the movement of slow particle is influenced by bridge to a greater extent. There is a discrepancy in between the analytical and numerical modes for small v_0 as the difference between the exact and the approximated capillary forces becomes significant when the particle inertia is small. The results presented in Figure 11 are in qualitative agreement with the literature.[15,20,22]

It can be seen from Figure 12 that $\bar{\varepsilon}$ increases with increasing value of $\pm|F_{ext}|$, the positive and negative signs

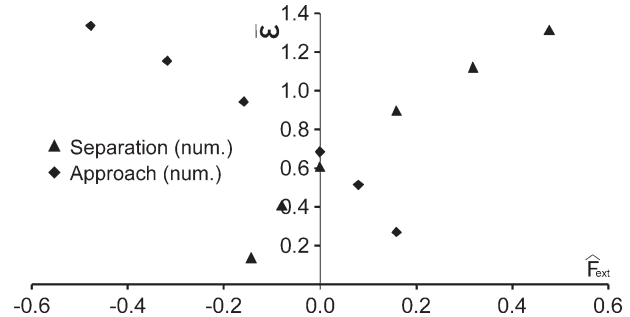

Figure 12. Fraction of residual relative momentum, $\bar{\varepsilon}$, as a function of the external force $\hat{F}_{ext}$.

$\xi_{min}=0.005$, $\hat{V}=3.19\cdot10^{-7}$, $Ca=0.029$, $v_0^A=-0.052$, $v_0^S=0.052$. Numerical prediction.

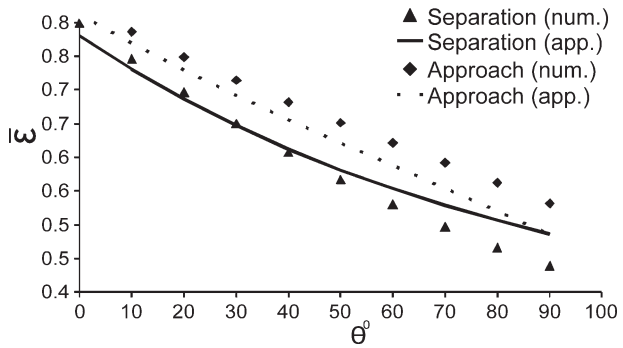

Figure 13. Fraction of residual relative momentum, $\bar{\varepsilon}$, as a function of the wetting angle θ.

$\xi_{min}=0.005$, $\hat{V}=3.19\cdot10^{-7}$, $C_a=0.029$, $\hat{F}_{ext}=0$, $v_0^A=-0.052$, $v_0^S=0.052$. Numerical results compared with the analytical, approximate solution.

applying to separation and approach, respectively. This stands to reason since F_{ext}, when acting in the same direction as the initial velocity, helps in maintaining the particle momentum in spite of the opposing viscous bridge force, while it acts with the viscous force to consume the momentum when oppositely directed to the initial velocity. This dependence is agreement with the results by Wang et al.[22]

The final study considered here illustrates the dependence of $\bar{\varepsilon}$ on the wetting angle, shown in Figure 13, presented in degrees for convenience. An increase in the wetting angle reduces the attraction of the particle by the bridge, which is one reason for the reduction of $\bar{\varepsilon}$ for the case of approach.

The opposite might have been expected for the case of separation, but the figure shows that $\bar{\varepsilon}$ also here decays with increasing wetting angle. This is explained by an increase in the maximum separation distance ξ_{max} (Eq. 14) with an increase in the wetting angle and, as a consequence, an increase in the distance over which the viscous force acts within the bridge. This latter result is in disagreement with Wang et al.[22] who found the time interval of separation to be reduced, and the final exit velocity to be higher, with an increase in the wetting angle, and the final exit velocity to be higher. However, the authors[22] did not apply an expression similar to Eq. 14.

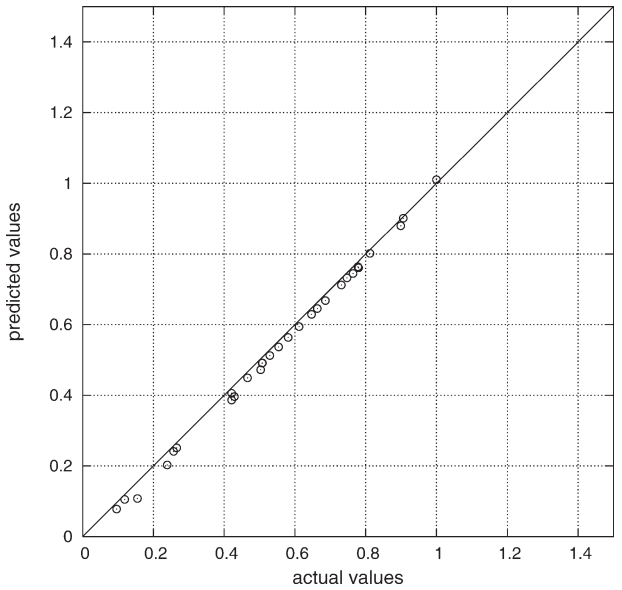

Figure 15. Fit of the analytical model to numerical results for the separation process.

An external force is not taken into account.

Fit of the Analytical Expressions to the Numerical Model

The existence of an analytical solution, which is in the satisfactory agreement with the numerical one makes it feasible to fit the analytical expression to the numerical model in order to create a semiempirical equation that can be implemented in simulations of particle collisions.

The most important difference between the analytical and the numerical models was found to be in the dependence on

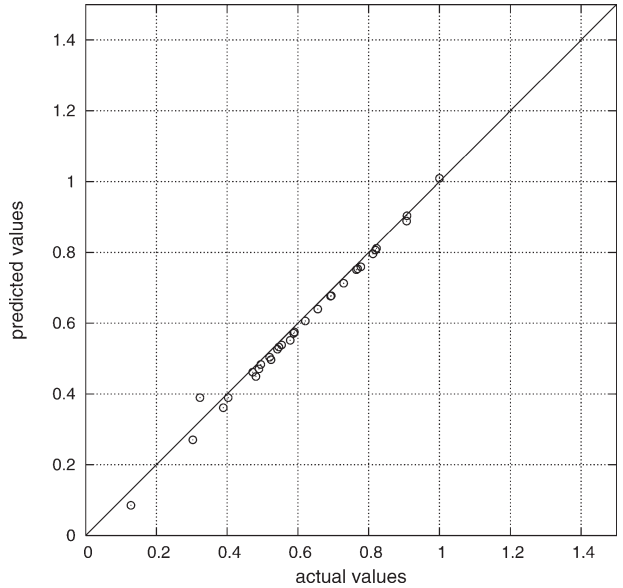

Figure 14. Fit of the analytical model to numerical results for the approach process.

An external force is not taken into account.

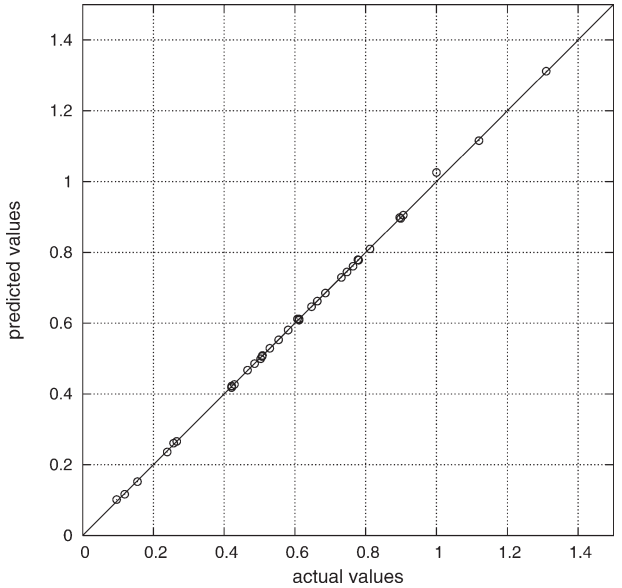

Figure 16. Fit of the analytical model to numerical results for the separation process.

An external force is taken into account.

the dimensionless bridge volume, $\hat{V}$, a parameter which was approximated in the analytical solution. Thus, when fitting the analytical model to the numerical one, all dependencies that are influenced by $\hat{V}$ should optimized by the fitting procedure. Accordingly, Eq. 14 is considered in the form

$$\tilde{\xi}_{\max} = b_1(1+0.5\theta)\left(1+(C_{a0})^{\frac{1}{2}}\right)\cdot \hat{V}^{a_1} \tag{31}$$

where a_1 and b_1 are fitting parameters, and the expression for φ, introduced to facilitate the analytical solution, is considered in the form

$$\tilde{\phi} = b_2 \frac{2}{3}\bar{\alpha}^{a_2}\cos\theta \tag{32}$$

with a_2 and b_2 fitting parameters. These expressions are then substituted into the analytical solutions:

$$\frac{v}{v_0^A} = 1+\frac{C_a}{v_0^A}\ln\left(\frac{\widetilde{\xi_{\max}}}{\xi_{\min}}\right)-\frac{\tilde{\phi}}{C_a v_0^A}\ln\left(-\left(C_a v_0^A\tilde{\phi}+1\right)\right)+\frac{\tilde{\phi}}{C_a v_0^A}$$
$$\times\ln\left[-1-C_a v_0^A\tilde{\phi}-C_a^2\tilde{\phi}\cdot\ln\left(\frac{\widetilde{\xi_{\max}}}{\xi_{\min}}\right)+\ln\left(-\left(C_a v_0\tilde{\phi}+1\right)\right)\right], \tag{33}$$

for approach and

$$\frac{v}{v_0^S} = 1+\frac{C_a}{v_0^S}\ln\left(\frac{\xi_{\min}}{\widetilde{\xi_{\max}}}\right)-\frac{\tilde{\phi}}{C_a v_0^S}\ln\left(C_a v_0^S\tilde{\phi}+1\right)$$
$$+\frac{\tilde{\phi}}{C_a v_0^S}\ln\left[1+C_a v_0^S\tilde{\phi}+C_a^2\tilde{\phi}\cdot\ln\left(\frac{\xi_{\min}}{\widetilde{\xi_{\max}}}\right)-\ln\left(C_a v_0^S\tilde{\phi}+1\right)\right] \tag{34}$$

for separation. The analytical solution thus has $b_1=b_2=1.0$ and $a_1=\frac{1}{3}$, $a_2=2.0$.

The fitting of the above expressions to a set of results from the numerical model was done using the multidimensional Rosenbrock search technique.[30] The analytical values for the fitting parameters were used as initial estimates. The result of the fitting was as follows. For the approach $a_1=0.331$, $b_1=1.000$, $a_2=2.000$, $b_2=1.001$ with Pearson's R equal to 0.99623. For the separation the fit parameters were $a_1=0.331$, $b_1=1.000$, $a_2=2.001$ and $b_2=1.000$ with Pearson's R equal to 0.99534. Parity plots for the fits are shown in Figures 14 and 15.

It is clear that the fit to the numerical model is very good and that the fitted equations are suitable for implementation in simulations involving particles that are cohesive due to bridging.

Equations 33,34 represent the mechanics of the bridge at the absence of an external force, and is, therefore, relevant for systems, such as pipe flow, where the particles are colliding with each other or the pipe wall, for example, to study agglomeration or particle deposition.

However, as mentioned in the introductory section, many experimental studies of bridge behavior are done by means of micromechanics, atomic-force microscopy or another technique which involves an external force acting to detach particles connected by a bridge. To compare the present models with such work it was deemed desirable also to fit the analytical expression to the numerical model with an external force acting, at least for the case of separation. To achieve this an optimization search for the case of separation (Eq. 34) was thus performed with an additional additive term representing the effect of an external force $\hat{F_{ext}}$

$$\frac{v}{v_0^S} = 1+\frac{C_a}{v_0^S}\ln\left(\frac{\xi_{\min}}{\widetilde{\xi_{\max}}}\right)-\frac{\tilde{\phi}}{C_a v_0^S}\ln\left(C_a v_0^S\tilde{\phi}+1\right)+\frac{\tilde{\phi}}{C_a v_0^S}$$
$$\times\ln\left[1+C_a v_0^S\tilde{\phi}+C_a^2\tilde{\phi}\cdot\ln\left(\frac{\xi_{\min}}{\widetilde{\xi_{\max}}}\right)-\ln\left(C_a v_0^S\tilde{\phi}+1\right)\right]+a_3\hat{F_{ext}}^{b_3} \tag{35}$$

The form of the term accounting for $\hat{F_{ext}}$ in Eq. 35 represents a constant term making the equation inhomogeneous, such that a particular solution of Eq. 23 will account for the effect of $\hat{F_{ext}}$.

The result of the fit is shown in Figure 16 for the case when the external force is taken into account. The parameters for the fit are $a_1=0.33053$, $b_1=0.966507$, $a_2=2.121788$, $b_2=1.65352518$, $a_3=0.810645$, $b_3=1.27359$. Pearson's R = 0.99984.

Conclusions

This article deals with collisions of particles affected by liquid bridging. It is suggested to model the process as taking place in tree stages:

- formation of the bridge and approach of the particles connected by the bridge,
- mechanistic contact of the particles, modeled by a classical hard-sphere collision model (this aspect is not discussed in this article, the equations are widely available, for example, in Ref. 13) and
- separation of the particles and breakage of the bridge.

Each of the stages are characterized by the fraction of normal relative momentum remaining after the dissipative processes taking place during the stage, $\bar{\varepsilon}$. The final normal component of the relative velocity of particle leaving the bridge is therefore given by

$$v = -v_0\bar{\varepsilon}_A\left(v_0^A\right)\bar{\varepsilon}_C\left(v(\xi_{\min})\right)\bar{\varepsilon}_S\left(v_0^S\right), \tag{36}$$

The effect of an external force on the collision has been investigated using a numerical model, and it has been shown that the particles may, in some cases, either

- reverse their normal motion before they even contact or
- agglomerate

under influence of the external force, depending on whether it acts to repel the particles or attract them to each other.

When the external force can be neglected, which is normally the case for colliding particles, an agglomeration criterion, Eq. 30, has been derived. It is derived by finding the separation, ξ_{crit}, at which the motion of the separating particles is reversed due to the effects of the bridge, and check whether this separation is one whereby the bridge is still in existence, that is, whether $\xi_{crit}\in(\xi_{\min},\xi_{\max})$. This criterion can also be used for estimating the probability of agglomeration ("collision efficiency") for the relevant flow systems.

If no agglomeration takes place the final velocity can be predicted with the use of the fractions of remaining relative momentum, $\bar{\epsilon}_A, \bar{\epsilon}_C$, and $\bar{\epsilon}_S$. Expressions for these parameters are derived in this article both using a more accurate model, which is solved numerically and using an approximate analytical model.

The existence of the analytical model made it possible to determine a "semiempirical" expression that accurately models the behavior of particles that collide with bridge formation.

This latter expression can be used in Eulerian-Lagrangian CFD models. In contrast to the discrete element-based approach, where the bridge-affected motion is resolved for each particle, this expression can be evaluated directly only once per collision, greatly reducing the computational costs of simulations.

Acknowledgments

The authors thank the Norwegian Research Council for funding via the FRINAT program.

Notation

$a_{1..3}, b_{1..3}$ = parameters of optimization
d_{sp} = height of spherical cap, m
F = force, N
g = acceleration due to gravity, m/s^2
K = integration constant
m = particle mass, kg
R = radius of particle, m
t = time, s
V = volume of the bridge, m^3
v = particle relative velocity, m/s
v^* = characteristic velocity, m/s
x = separation distance, m

Greek letters

α = filling angle
$\bar{\alpha}$ = mean filling angle
$\bar{\varepsilon}$ = fraction of relative momentum remaining
ϕ = intermediate variable
$\hat{\phi}$ = approximated intermediate variable
γ = surface tension, N/m
μ = dynamic viscosity, Pa s
ρ = density, kg/m^3
θ = wetting angle

Dimensionless values

$C_a = \frac{3\mu v*}{\gamma}$ = capillary number of the bridge
$C_{a0} = \frac{C_a v_0}{3}$ = capillary number as in Pitois et al.
$\hat{F} = \frac{F}{\pi R \gamma}$ = dimensionless force
$\hat{V}$ = dimensionless bridge volume
v = dimensionless velocity
ξ = dimensionless separation distance
$\widetilde{\xi_{max}}$ = approximated maximum separation distance

Subscripts, superscripts

A = approach
C = contact collision
c = capillary
crit = critical (agglomeration event)
d = dissipative
ext = external
M = equivalent to Mazzone et al.
max = maximum
min = minimum
R–P = Rayleigh—Plateau instability
S = separation
0 = initial
1, 2 = numbers of particles interacting

Literature Cited

1. Seville JPK, Willett CD, Knight PC. Interparticle forces in fluidisation: a review. *Powder Technol*. 2000;113:261–268.
2. Liu LX, Litster JD, Iveson SM, Ennis BJ. Coalescence of deformable granules in wet granulation processes. *AIChE J*. 2000;46:529–539.
3. Bouffard J, Cabana A, Chaouki J, Bertrand F. Experimental investigation of the effect of particle cohesion on the flow dynamics in a spheronizer. *AIChE J*. 2013;59(5):1491–1501.
4. Chua KW, Makkawi YT, Hounslow MJ. Time scale analysis for fluidized bed melt granulation-II: binder spreading rate. *Chem Eng Sci*. 2011;66:327–335.
5. Anklam MR, York JD, Helmerich L, Firoozabadi A. Effects of anti-agglomerants on the interactions between hydrate particles. *AIChE J*. 2012;54:565–574.
6. Balakin BV, Kosinski P, Hoffmann AC. Experimental study and computational fluid dynamics modeling of deposition of hydrate particles in a pipeline with turbulent water flow. *Chem Eng Sci*. 2011; 66:755–765.
7. Aman ZM, Joshi SE, Sloan ED, Sum AK, Koh CA. Micromechanical cohesion force measurements to determine cyclopentane hydrate interfacial properties. *J Colloid Interface Sci*. 2012;376:283–288.
8. Mazzone DN, Tardos GI, Pfeffer R. The behavior of liquid bridges between two relatively moving particles. *Powder Technol*. 1987;51: 71–83.
9. Pitois O, Moucheront P, Chateau X. Rupture energy of a pendular liquid bridge. *Eur Phys J B*. 2001;23:79–86.
10. Mikami T, Kamiya H, Horio M. Numerical simulation of cohesive powder behavior in a fluidized bed. *Langmuir*. 2005;21:1927–1940.
11. Rabinovich YI, Esayanur MS, Moudgil BM. Capillary forces between two spheres with a fixed volume liquid bridge: theory and experiment. *Chem Eng Sci*. 1998;53:10992–10997.
12. Israelachvili JN. Intermolecular and Surface Forces, Second Edition: With Applications to Colloidal and Biological Systems. New York: Academic Press, 1992.
13. Crowe C, Sommerfeld M, Tsuji Y. Multiphase Flows with Droplets and Particles. Boca Raton: CRC Press, 1998.
14. Ennis BJ, Tardos G, Pfeffer R. A microlevel-based characterization of granulation phenomena. *Powder Technol*. 1991;65:257–272.
15. Antonyuk S, Heinrich S, Deen NG, Kuipers JAM. Influence of liquid layers on energy absorption during particle impact. *Particuology*. 2009;7:245–249.
16. Jen CO, Tsao KC. Coal-ash agglomeration mechanism and its application in high temperature cyclones. *Sep Sci Technol*. 1980;15:263–276.
17. Zhang W, Noda R, Horio M. Evaluation of lubrication force on colliding particles for DEM simulation of fluidized beds. *Powder Technol*. 2005;158:92–101.
18. Gollwitzer F, Rehberg I, Huang K, Kruelle CA. Coefficient of restitution for wet particles. *arXiv.org >cond-mat>arXiv:1202.1750v1*, 2012, 1–10.
19. Jain D, Deen NG, Kuipers JAM, Antonyuk S, Heinrich S. Direct numerical simulation of particle impact on thin liquid films using a combined volume of fluid and immersed boundary method. *Chem Eng Sci*. 2012;69:530–540.
20. Davis RH, Rager DA, Good BT. Elastohydrodynamic rebound of spheres from coated surfaces. *J Fluid Mech*. 2002;468:107–119.
21. Midi GDR. On dense granular flows. *Eur Phys Rev E*. 2004;14:341–365.
22. Wang L, Rong W, Guo B, Huang G, Sun L. Dynamic separation of a sphere from a flat or sphere in the presence of a liquid meniscus. *Tribol Trans*. 2011;54:542–547.
23. Balakin B, Hoffmann AC, Kosinski P. The collision efficiency in a shear flow. *Chem Eng Sci*. 2012;68:305–312.
24. Lian G, Thornton C, Adams MJ. Discrete particle simulation of agglomerate impact coalescence. *Chem Eng Sci*. 1998;53:3381–3391.
25. Megias-Alguacil D, Gauckler LJ. Capillary forces between two solid spheres linked by a concave liquid bridge: regions of existence and forces mapping. *AIChE J*. 2009;55:1103–1109.
26. Darabi P, Pougatch K, Salcudean M, Grecov D. A novel coalescence model for binary collision of identical wet particles. *Chem Eng Sci*. 2009;64:1868–1876.
27. Zaitsev VF, Polyanin AD. Handbook of Exact Solutions for Ordinary Differential Equations. Boca Raton: Chapman and Hall/CRC, 2003.
28. Corless RM, Gonnet GH, Hare DEG, Jeffrey DJ, Knuth DE. On the Lambert W function. *Adv Comput Math*. 1996;5:329–359.
29. Chapeau-Blondeau F, Monir A. Numerical evaluation of the Lambert W function and application to generation of generalized gaussian noise with exponent 1/2. *IEEE Trans Signal Process*. 2002;50(9): 2160–2165.
30. Conn AR, Gould NIM, Toint PL. Testing a class of methods for solving minimization problems with simple bounds on the variables. *Math Comput*. 1988;50:399–430.

Appendix: Restitution in Tangential Direction

To obtain a complete model for particle collisions with bridge formation, it is necessary also to consider the dissipative shear force acting in the bridge. The present approach is based on using the equations developed in the main text to estimate the loss of momentum during the approach and separation stages, and allow the particles to undergo a collision in accordance with the classical hard-sphere model between these two stages. The classical hard-sphere model also involves dissipation of relative momentum due to a normal coefficient of restitution that is less than unity and a tangential frictional force, described as Coulombian friction. In this appendix, estimates for the tangential friction acting in the bridge during approach and separation and the Coulombian friction acting during the hard-sphere collision are compared. The loss of the particle initial energy within the bridge in tangential direction can be estimated from the work done by the dissipative force within the bridge

$$\frac{mv_{\tau,0}^2}{2}-\frac{mv_{\tau}^2}{2}=\left(F_{\mathrm{d},\tau}^{\max}+F_{\tau,\mathrm{ext}}\right)R\alpha_{\max} \tag{A1}$$

where v_τ is the tangential component of the particle relative velocity and $F_{\tau,\mathrm{ext}}$ is the tangential component of the external force. It is here assumed, as an approximation that the force acts over a distance equal to the diameter of the bridge. The maximum possible value of tangential component of the dissipative force acting in the bridge, $F_{\mathrm{d},\tau^{\max}}$, is taken as the shear force acting at the minimum particle separation

$$F_{\mathrm{d},\tau}^{\max}=-A\mu\frac{dv_{\tau}}{dx}\approx A\mu\frac{v_{\tau}}{x_{\min}} \tag{A2}$$

where $A\approx\pi R^2\alpha_{\max}^2$ is the area of the particle covered by the bridge at the separation $x_{\min}$. Scaling Eq. A1 with $\frac{mv^*}{2}$ and substituting $x_{\min}=\xi_{\min}R$, $v_\tau=v_\tau v^*$ it becomes dimensionless

$$v_{\tau,0}^2-v_{\tau}^2=-\frac{2}{3}\frac{C_{\mathrm{a}}\alpha_{\max}^3 v_{\tau}}{\xi_{\min}}+\frac{2F_{\tau,\mathrm{ext}}R\alpha_{\max}}{mv^{*2}} \tag{A3}$$

Solving this equation with respect to v_τ and scaling it with $v_{\tau,0}$, the remaining relative tangential momentum of the particles after the collision is found as

$$\bar{\varepsilon_{\tau}}=\frac{1}{2v_{\tau,0}}\left(\frac{2}{3}\frac{C_{\mathrm{a}}\alpha_{\max}^3}{\xi_{\min}}+\sqrt{\frac{4}{9}\left(\frac{C_{\mathrm{a}}\alpha_{\max}^3}{\xi_{\min}}\right)^2+4\left(v_{\tau,0}^2-\frac{2F_{\tau,\mathrm{ext}}R\alpha_{\max}}{mv^{*2}}\right)}\right) \tag{A4}$$

The resulting reduction of momentum in the tangential direction is less than 1% for the values of dimensionless variables used in the current paper. In this approximation, the particle rotation generated as a result of the tangential stress in the bridge has been neglected, if this had been accounted for the loss in linear momentum is likely to have been less. For the purpose of comparison the collision of two "dry" noncohesive particles that were not rotating before the collision, under an angle of 45 was modeled using a classical hard-sphere model (given in Crowe et al.[13]). A normal coefficient of restitution of 1.0 and a Coulombian friction factor of 0.15 (a typical value) were used, the physical parameters of the particles were the same as above. In this collision, the particles lost 29% of their relative tangential momentum. In most cases, the loss of tangential momentum due to the effects in the bridge is therefore likely to be small compared to that due to friction during the actual particle contact.

Manuscript received Feb. 25, 2013, and revision received May 16, 2013.